Contents

Chapter 20

Waves in Cold Plasmas: Two-Fluid Formalism

Version 1020.1.K.pdf, 08 April 2009.
Please send comments, suggestions, and errata via email to kip@caltech.edu or on paper to Kip Thorne, 350-17 Caltech, Pasadena CA 91125

Box 20.1
Reader's Guide

- This chapter relies significantly on:
  - Chapter 19 on the particle kinetics of plasmas.
  - The basic concepts of fluid mechanics, Secs. 12.4 and 12.5.
  - Magnetosonic waves, Sec. 17.7.
  - The basic concepts of geometric optics, Secs. 6.2 and 6.3
- The remaining chapters 21 and 22 of Part V, Plasma Physics, rely heavily on this chapter.

20.1 Overview

The growth of plasma physics came about historically through the studies of oscillations in electric discharges and the contemporaneous development of the means to broadcast radio waves over increasing distances by reflecting them off a layer of partially ionized gas in the upper atmosphere known as the *ionosphere*. It is therefore not surprising that most early research was devoted to describing the different modes of wave propagation. Even in the simplest, linear approximation, we will see that the variety of possible modes is immense. In the previous section, we have introduced several length and time scales, e.g. the gyro radius

and Debye length, the plasma period, the gyro period and the collision frequency. To these must now be added the wavelength and period of the wave under study. The relative ordering of these different scales controls the characteristics of the waves, and it is already apparent that there are a bewildering number of possibilities. If we further recognize that plasmas are collisionless and that there is no guarantee that the particle distribution functions can be characterized by a single temperature, then the possibilities multiply.

Fortunately, the techniques needed to describe the propagation of linear wave perturbations in a particular equilibrium configuration of a plasma are straightforward and can be amply illustrated by studying a few simple cases. In this section, we shall follow this course by restricting our attention to one class of modes, those where we can either ignore completely the thermal motions of the ions and electrons that comprise the plasma (in other words treat these species as *cold*) or include them using just a velocity dispersion or temperature. We can then apply our knowledge of fluid dynamics by treating the ions and electrons separately as fluids, upon which act electromagnetic forces. This is called the *two-fluid formalism* for plasmas. In the next chapter, we shall show when and how waves are sensitive to the actual distribution of particle speeds by developing the more sophisticated *kinetic-theory formalism* and using it to study waves in *warm plasmas*.

We begin our two-fluid study of plasma waves in Sec. 20.2 by deriving a very general wave equation, which governs weak waves in a homogeneous plasma that may or may not have a magnetic field, and also governs electromagnetic waves in any other dielectric medium. That wave equation and the associated dispersion relation for the wave modes depend on a dielectric tensor, which must be derived from an examination of the motion of the electrons and protons (or other charge carriers) inside the wave.

In Sec. 20.3 we specialize to wave modes in a uniform, unmagnetized plasma. Using a two-fluid (electron-fluid and proton-fluid) description of the charge-carriers' motions, we derive the dielectric tensor and thence the dispersion relation for the wave modes. The modes fall into two classes: (i) *Transverse or electromagnetic modes*. These are modified versions of electromagnetic waves in vacuum. As we shall see, they can propagate only at frequencies above the plasma frequency; at lower frequencies they become evanescent. (ii) *Longitudinal waves*, which come in two species: *Langmuir waves* and *ion acoustic waves*. Longitudinal waves are a melded combination of sound waves in a fluid and electrostatic plasma oscillations; their restoring force is a mixture of thermal pressure and electrostatic forces.

In Sec. 20.4, we explore how a uniform magnetic field changes the character of these waves. The $\mathbf{B}$ field makes the plasma anisotropic but axially symmetric. As a result, the dielectric tensor, dispersion relation, and wave modes have much in common with those in an anisotropic but axially symmetric dielectric crystal, which we studied in the context of nonlinear optics in Chap. 9. A plasma, however, has a much richer set of characteristic frequencies than does a crystal (electron plasma frequency, electron cyclotron frequency, ion cyclotron frequency, ...). As a result, even in the regime of weak linear waves and a cold plasma (no thermal pressure), the plasma has a far greater richness of modes than does a crystal.

In Sec. 20.4 we derive the general dispersion relation that encompasses all of these cold-magnetized-plasma modes, and explore the special cases of modes that propagate parallel to

and perpendicular to the magnetic field. Then in Sec. 20.5 we examine a practical example: the propagation of radio waves in the Earth's ionosphere, where it is a good approximation to ignore the ion motion and work with a one-fluid (i.e. electron-fluid) theory. Having gained insight into simple cases (parallel modes, perpendicular modes, and one-fluid modes), we return in Sec. 20.6 to the full class of linear modes in a cold, magnetized two-fluid plasma and briefly describe some tools by which one can make sense of them all.

Finally, in Sec. 20.7 we turn to the question of plasma stability. In Part IV we saw that fluid flows that have sufficient shear are unstable; perturbations can feed off the relative kinetic energy of adjacent regions of the fluid, and use that energy to power an exponential growth. In plasmas, with their long mean free paths, there can similarly exist kinetic energies of relative, ordered, motion in velocity space; and perturbations, feeding off those energies, can grow exponentially. To study this in full requires the kinetic-theory description of a plasma, which we develop in Chap. 21; but in Sec. 20.7 we get insight into a prominent example of such a velocity-space instability by analyzing two cold plasma streams moving through each other. We illustrate the resulting *two-stream instability* by a short discussion of particle beams that are created in disturbances on the surface of the sun and propagate out through the solar wind.

20.2 Dielectric Tensor, Wave Equation, and General Dispersion Relation

We begin our study of waves in plasmas by deriving a very general wave equation which applies equally well to electromagnetic waves in unmagnetized plasmas, in magnetized plasmas, and in any other kind of dielectric medium such as an anisotropic crystal. This wave equation is the same one as we used in our study of nonlinear optics in Chap. 9 [Eqs. (9.38) and (9.39a)], and the derivation is essentially the same as that sketched in Exercise 9.6:

When a wave propagates through a plasma (or other dielectric), it entails a relative motion of electrons and protons (or other charge carriers). Assuming the wave has small enough amplitude to be linear, those charge motions can be embodied in an oscillating polarization (electric dipole moment per unit volume) $\mathbf{P}(\mathbf{x}, t)$, which is related to the plasma's (or dielectric's) varying charge density ρ_e and current density $\mathbf{j}$ in the usual way

$$\boxed{\rho_e = -\boldsymbol{\nabla}\cdot\mathbf{P}\ , \quad \mathbf{j} = \frac{\partial \mathbf{P}}{\partial t}\ .} \tag{20.1}$$

(These relations enforce charge conservation, $\partial\rho_e/\partial t + \boldsymbol{\nabla}\cdot\mathbf{j} = 0$.) When these ρ_e and $\mathbf{j}$ are inserted into the standard Maxwell equations for $\mathbf{E}$ and $\mathbf{B}$, one obtains

$$\boxed{\boldsymbol{\nabla}\cdot\mathbf{E} = -\frac{\boldsymbol{\nabla}\cdot\mathbf{P}}{\epsilon_0}\ , \quad \boldsymbol{\nabla}\cdot\mathbf{B} = 0\ , \quad \boldsymbol{\nabla}\times\mathbf{E} = -\frac{\partial\mathbf{B}}{\partial t}\ , \quad \boldsymbol{\nabla}\times\mathbf{B} = \mu_0\frac{\partial\mathbf{P}}{\partial t} + \frac{1}{c^2}\frac{\partial\mathbf{E}}{\partial t}\ .} \tag{20.2}$$

If the plasma is endowed with a uniform magnetic field $\mathbf{B}_o$, that field can be left out of these equations, as its divergence and curl are guaranteed to vanish. Thus, we can regard $\mathbf{E}$, $\mathbf{B}$ and $\mathbf{P}$ in these Maxwell equations as the perturbed quantities associated with the waves.

From a detailed analysis of the response of the charge carriers to the oscillating **E** and **B** fields, one can deduce a linear relationship between the waves' electric field **E** and the polarization **P**,

$$\boxed{P_j = \epsilon_o \chi_{jk} E_k \ .} \tag{20.3}$$

Here ϵ_0 is the vacuum permitivity and χ_{jk} is a dimensionless, tensorial electric susceptibility [cf. Eq. (9.21)]. A different, but equivalent, viewpoint on the relationship between **P** and **E** can be deduced by taking the time derivative of Eq. (20.3), setting $\partial \mathbf{P}/\partial t = \mathbf{j}$, assuming a sinusoidal time variation $e^{-i\omega t}$ so $\partial \mathbf{E}/\partial t = -i\omega \mathbf{E}$, and then reinterpreting the result as Ohm's law with a tensorial electric conductivity $\kappa_{\mathrm{e}\,jk}$:

$$\boxed{j_j = \kappa_{\mathrm{e}\,jk} E_k \ , \quad \kappa_{\mathrm{e}\,jk} = -i\omega \epsilon_0 \chi_{jk} \ .} \tag{20.4}$$

Evidently, for sinusoidal waves the electric susceptibility χ_{jk} and the electric conductivity $\kappa_{\mathrm{e}\,jk}$ embody the same information about the wave-particle interactions.

That information is also embodied in a third object: the dimensionless dielectric tensor ϵ_{jk}, which relates the electric displacement **D** to the electric field **E**:

$$\boxed{D_j \equiv \epsilon_0 E_j + P_j = \epsilon_0 \epsilon_{jk} E_k \ , \quad \epsilon_{jk} = \delta_{jk} + \chi_{jk} = \delta_{jk} + \frac{i}{\epsilon_0 \omega} \kappa_{\mathrm{e}\,jk} \ .} \tag{20.5}$$

In the next section we shall derive the value of the dielectric tensor ϵ_{jk} for waves in an unmagnetized plasma, and in Sec. 20.3 we shall derive it for a magnetized plasma.

Using the definition $\mathbf{D} = \epsilon_0 \mathbf{E} + \mathbf{P}$, we can eliminate **P** from equations (20.2), thereby obtaining the familiar form of Maxwell's equations for dielectric media with no non-polarization-based charges or currents:

$$\boldsymbol{\nabla} \cdot \mathbf{D} = 0 \ , \quad \boldsymbol{\nabla} \cdot \mathbf{B} = 0 \ , \quad \boldsymbol{\nabla} \times \mathbf{E} = -\frac{\partial \mathbf{B}}{\partial t} \ , \quad \boldsymbol{\nabla} \times \mathbf{B} = \mu_0 \frac{\partial \mathbf{D}}{\partial t} \ . \tag{20.6}$$

By taking the curl of the third of these equations and combining with the fourth and with $D_j = \epsilon_0 \epsilon_{jk} E_k$, we obtain the wave equation that governs the perturbations:

$$\nabla^2 \mathbf{E} - \boldsymbol{\nabla}(\boldsymbol{\nabla} \cdot \mathbf{E}) - \boldsymbol{\epsilon} \cdot \frac{1}{c^2} \frac{\partial^2 \mathbf{E}}{\partial t^2} = 0 \ , \tag{20.7}$$

where $\boldsymbol{\epsilon}$ is our index-free notation for ϵ_{jk}. Specializing to a plane-wave mode with wave vector **k** and angular frequency ω, so $\mathbf{E} \propto e^{i\mathbf{k}\mathbf{x}} e^{-i\omega t}$, we convert this wave equation into a homogeneous algebraic equation for the Cartesian components of the electric vector E_j (cf. Box 11.2):

$$\boxed{L_{ij} E_j = 0 \ .} \tag{20.8}$$

where

$$\boxed{L_{ij} = k_i k_j - k^2 \delta_{ij} + \frac{\omega^2}{c^2} \epsilon_{ij} \ .} \tag{20.9}$$

The algebratized wave equation (20.8) can have a solution only if the determinant of the three-dimensional matrix L_{ij} vanishes:

$$\boxed{\det||L_{ij}|| \equiv \det\left|\left|k_i k_j - k^2\delta_{ij} + \frac{\omega^2}{c^2}\epsilon_{ij}\right|\right| .} \tag{20.10}$$

For a plasma this will be a polynomial equation for the angular frequency as a function of the wave vector (with ω and $\mathbf{k}$ appearing not only explicity in L_{ij} but also implicitly in the functional form of ϵ_{jk}). Each solution, $\omega(\mathbf{k})$, of this equation will be the dispersion relation for a particular wave mode. We therefore can regard Eq. (20.10) as the general dispersion relation for plasma waves—and for linear electromagnetic waves in any other kind of dielectric medium.

To obtain an explicit form of the dispersion relation (20.8), we must give a prescription for calculating the dielectric tensor ϵ_{ij}, or equivalently the conductivity tensor $\kappa_{\mathrm{e}\,ij}$ or the-susceptibility tensor χ_{ij}. The simplest prescription involves treating the electrons and ions as independent fluids.

20.3 Wave Modes in an Unmagnetized Plasma

20.3.1 Two-Fluid Formalism

We now specialize to waves in a homogeneous, unmagnetized electron-proton plasma. The plasma necessarily contains rapidly moving electrons and ions, and their individual responses to an applied electromagnetic field depend on their velocities. In the simplest model of this response, we average over all the particles in a species (electrons or protons in this case) and treat them collectively as a fluid. Now, the fact that all the electrons are treated as one fluid does not mean that they have to collide with one another many times in each wave period. In fact, as we have already emphasized in Chap. 19, electron-electron collisions are usually quite rare and we usually ignore them. Nevertheless, we can still define a mean fluid velocity for both the electrons and the protons by averaging over their total velocity distribution functions just as we would for a gas:

$$\boxed{\mathbf{u}_s = \langle \mathbf{v} \rangle_s \; ; \quad s = p, e \; ,} \tag{20.11}$$

where the subscripts p and e refer to protons and electrons. Similarly, for each fluid we define a pressure tensor using the fluid's dispersion of particle velocities:

$$\boxed{\mathbf{P}_s = n_s m_s \langle (\mathbf{v} - \mathbf{u}_s) \otimes (\mathbf{v} - \mathbf{u}_s) \rangle} \tag{20.12}$$

[cf. Eqs. 18.42) and (18.43)].

Consider, first, the unperturbed plasma in the absence of a wave and work in a frame in which the proton fluid velocity $\mathbf{u}_p$ vanishes. By assumption the equilibrium is spatially uniform. Therefore there can be no spatial variation in the electric field and no net charge density. (If there were an electric field, then charges would quickly flow to neutralize it.)

Therefore, the electron density must equal the proton density. Furthermore, there can be no net current as this would lead to a variation in the magnetic field, so since the proton current vanishes, the electron current $= -en_e\mathbf{u}_e$ must also vanish and the electron fluid velocity $\mathbf{u}_e$ must also vanish in our chosen frame.

Now apply an electromagnetic perturbation. This will induce a small, oscillating fluid velocity $\mathbf{u}_s$ in both the proton and electron fluids. It should not worry us that the fluid velocity is small compared with the random speeds of the constituent particles; the same is true in any subsonic gas dynamical flow, but the fluid description remains good there and so also here.

The oscillating density n_s and oscillating mean velocity $\mathbf{u}_s$ of each species s must satisfy the equation of continuity (particle conservation)

$$\boxed{\frac{\partial n_s}{\partial t} + \boldsymbol{\nabla}\cdot(n_s\mathbf{u}_s) = 0} \tag{20.13}$$

and the equation of motion (momentum conservation—Euler equation with Lorentz force added to the right side)

$$\boxed{n_s m_s\left(\frac{\partial \mathbf{u}_s}{\partial t} + (\mathbf{u}_s\cdot\nabla)\mathbf{u}_s\right) = -\boldsymbol{\nabla}\cdot\mathbf{P}_s + n_s q_s(\mathbf{E}+\mathbf{u}_s\times\mathbf{B})\,.} \tag{20.14}$$

In these equations and below, $q_s = \pm e$ is the particles' charge (positive for protons and negative for electrons). Note that, as collisions are ineffectual, we cannot assume that the pressure tensor is isotropic.

20.3.2 Dielectric Tensor and Dispersion Relation for a Cold Plasma

Continuing to keep the plasma unmagnetized, let us further simplify matters (temporarily) by restricting ourselves to a cold plasma, so the tensorial pressures vanish, $\mathbf{P}_s = 0$. As we are only interested in linear wave modes, we rewrite Eqs. (20.13), (20.14) just retaining terms that are first order in perturbed quantities, i.e. dropping the $(\mathbf{u}_s\cdot\boldsymbol{\nabla})\mathbf{u}_s$ and $\mathbf{u}_s\times\mathbf{B}$ terms. Then, focusing on a plane-wave mode, $\propto \exp[i(\mathbf{k}\cdot\mathbf{x}-\omega t)]$, we bring the equation of motion (20.14) into the form

$$\boxed{-i\omega n_s m_s\mathbf{u}_s = q_s n_s\mathbf{E}} \tag{20.15}$$

for each species, $s = p, e$. From this, we can immediately deduce the linearized current density

$$\mathbf{j} = \sum_s n_s q_s\mathbf{u}_s = \sum_s \frac{in_s q_s^2}{m_s\omega}\mathbf{E}\,, \tag{20.16}$$

from which we infer that the conductivity tensor $\boldsymbol{\kappa}_{\rm e}$ has Cartesian components

$$\kappa_{{\rm e}\,ij} = \sum_s \frac{in_s q_s^2}{m_s\omega}\delta_{ij}\,, \tag{20.17}$$

where δ_{ij} is the Kronecker delta. Note that the conductivity is purely imaginary, which means that the current oscillates out of phase with the applied electric field, which in turn

implies that there is no time-averaged ohmic energy dissipation, $\langle \mathbf{j} \cdot \mathbf{E} \rangle = 0$. Inserting the conductivity tensor (20.17) into the general equation (20.5) for the dielectric tensor, we obtain

$$\epsilon_{ij} = \delta_{ij} + \frac{i}{\epsilon_0 \omega} \kappa_{\mathrm{e}\, ij} = \left(1 - \frac{\omega_p^2}{\omega^2}\right) \delta_{ij} \ . \tag{20.18}$$

Here and throughout this chapter, the plasma frequency ω_p is very slightly different from that used in Chap. 19: it includes a tiny (1/1860) correction due to the motion of the protons, which was neglected in the analysis of plasma oscillations in Sec. 18.3.3:

$$\boxed{\omega_p^2 = \sum_s \frac{n_s q_s^2}{m_s \epsilon_0} = \frac{n e^2}{m_e \epsilon_0} \left(1 + \frac{m_e}{m_p}\right) \ .} \tag{20.19}$$

Note that because there is no physical source of a preferred direction in the plasma, the dielectric tensor (20.18) is isotropic.

Now let the waves propagate in the z direction, without loss of generality, so $\mathbf{k} = k\mathbf{e}_z$. Then the algebratized wave operator (20.9), with $\boldsymbol{\epsilon}$ given by (20.18), takes the following form:

$$\boxed{L_{ij} = \frac{\omega^2}{c^2} \begin{pmatrix} 1 - \frac{c^2 k^2}{\omega^2} - \frac{\omega_p^2}{\omega^2} & 0 & 0 \\ 0 & 1 - \frac{c^2 k^2}{\omega^2} - \frac{\omega_p^2}{\omega^2} & 0 \\ 0 & 0 & 1 - \frac{\omega_p^2}{\omega^2} \end{pmatrix} \ .} \tag{20.20}$$

The corresponding dispersion relation $\det||L_{jk}||$ becomes

$$\left(1 - \frac{c^2 k^2}{\omega^2} - \frac{\omega_p^2}{\omega^2}\right)^2 \left(1 - \frac{\omega_p^2}{\omega^2}\right) = 0 \ . \tag{20.21}$$

This is a polynomical equation of order 6 for ω as a function of k, so formally there are six solutions corresponding to three pairs of modes propagating in opposite directions.

Two of the pairs of modes are degenerate with frequency

$$\boxed{\omega = \sqrt{\omega_p^2 + c^2 k^2} \ .} \tag{20.22}$$

We shall study them in the next subsection. The remaining pair of modes exist at a single frequency,

$$\boxed{\omega = \omega_p \ .} \tag{20.23}$$

These must be the electrostatic plasma oscillations that we studied in Sec. 18.3.3, (though now with an arbitrary wave number k while in Sec. 18.3.3 the wave number was assumed zero.) In Sec. 20.3.4 we shall show that this is so and shall explore how these plasma oscillations get modified by finite-temperature effects.

20.3.3 Electromagnetic Plasma Waves

To learn the physical nature of the modes with dispersion relation $\omega = \sqrt{\omega_p^2 + c^2k^2}$ [Eq. (20.22)], we must examine the details of their electric-field oscillations, magnetic-field oscillations, and electron and proton motions. The first key to this is the algebratized wave equation $L_{ij}E_j = 0$, with L_{ij} specialized to the dispersion relation (20.22): $||L_{ij}|| = \mathrm{diag}[0, 0, (\omega^2 - \omega_p^2)/c^2]$. In this case the general solution to $L_{ij}E_j = 0$ is an electric field that lies in the x–y plane (transverse plane), i.e. that is orthogonal to the waves' propagation vector $\mathbf{k} = k\mathbf{e}_z$. The third of the Maxwell equations (20.2) implies that the magnetic field is

$$\mathbf{B} = (\mathbf{k}/\omega) \times \mathbf{E} \,, \tag{20.24}$$

which also lies in the transverse plane and is orthogonal to $\mathbf{E}$. Evidently, these modes are close analogs of electromagnetic waves in vacuum; correspondingly, they are known as the plasma's *electromagnetic modes*. The electron and proton motions in these modes, as given by Eq. (20.15), are oscillatory displacements in the direction of $\mathbf{E}$ but out of phase with $\mathbf{E}$. The amplitudes of the fluid motions vary as $1/\omega$; as one decreases ω, the fluid amplitudes grow.

The dispersion relation for these modes, Eq. (20.22), implies that they can only propagate (i.e. have real angular frequency when the wave vector is real) if ω exceeds the plasma frequency. As ω is decreased toward ω_p, $k \to 0$ so these modes become electrostatic plasma oscillations with arbitrarily long wavelength orthogonal to the oscillation direction, i.e., they become a spatially homogeneous variant of the plasma oscillations studied in Sec. 18.3.3. At $\omega < \omega_p$ these modes become evanescent.

In their regime of propagation, $\omega > \omega_p$, these cold-plasma electromagnetic waves have a phase velocity given by

$$\mathbf{V}_{\rm ph} = \frac{\omega}{k}\hat{\mathbf{k}} = c\left(1 - \frac{\omega_p^2}{\omega^2}\right)^{-1/2}\hat{\mathbf{k}} \,, \tag{20.25}$$

where $\hat{\mathbf{k}} \equiv \mathbf{k}/k$ is a unit vector in the propagation direction. Although this phase velocity exceeds the speed of light, causality is not violated because information (and energy) propagate at the group velocity, not the phase velocity. The group velocity is readily shown to be

$$\mathbf{V}_g = \frac{\partial\omega}{\partial\mathbf{k}} = \frac{c^2\mathbf{k}}{\omega} = c\left(1 - \frac{\omega_p^2}{\omega^2}\right)^{1/2}\hat{\mathbf{k}} \,, \tag{20.26}$$

which is less than c.

These cold-plasma electromagnetic modes transport energy and momentum just like wave modes in a fluid. There are three contributions to the waves' mean (time-averaged) energy density: the electric, the magnetic and the kinetic energy densities. (If we had retained the pressure then there would have been an additional contribution from the internal energy.) In order to compute these mean energy densities, we must form the time average of products of physical quantities. Now, we have used the complex representation to denote each of our oscillating quantities (e.g. E_x), so we must be careful to remember that $Ae^{i(\mathbf{k}\cdot\mathbf{x}-\omega t)}$ is an abbreviation for the real part of this quantity—which is the physical A. It is easy to show

that the time-averaged value of the physical A times the physical B (which we shall denote by $\langle AB\rangle$) is given in terms of their complex amplitudes by

$$\langle AB\rangle = \frac{AB^* + A^*B}{4} \ . \tag{20.27}$$

Using Eqs. (20.24) and (20.25), we can write the magnetic energy density in the form $\langle B^2\rangle/2\mu_0 = (1-\omega_p^2/\omega^2)\epsilon_0\langle E^2\rangle/2$. Using Eq. (20.16), the electron kinetic energy is $n_e m_e\langle u_e^2\rangle/2 = (\omega_{pe}^2/\omega^2)\epsilon_0\langle E^2\rangle/2$ and likewise for the proton kinetic energy. Summing these contributions and using Eq. (20.27), we obtain

$$\begin{aligned} U &= \frac{\epsilon_0 EE^*}{4} + \frac{BB^*}{4\mu_0} + \sum_s \frac{n_s m_s u_s u_s^*}{4} \\ &= \frac{\epsilon_0 EE^*}{2} \ . \end{aligned} \tag{20.28}$$

The mean energy flux in the wave is carried (to quadratic order) by the electromagnetic field and is given by the Poynting flux. (The kinetic-energy flux vanishes to this order.) A straightforward calculation gives

$$\begin{aligned} \mathbf{S} = \langle \mathbf{E}\times\mathbf{B}\rangle &= \frac{\mathbf{E}\times\mathbf{B}^* + \mathbf{E}^*\times\mathbf{B}}{4} = \frac{EE^*\mathbf{k}}{2\mu_0\omega} \\ &= UV_g \ , \end{aligned} \tag{20.29}$$

where we have used $\mu_0 = c^{-2}\epsilon_0^{-1}$. We therefore find that the energy flux is the product of the energy density and the group velocity, as is true quite generally; cf. Sec. 6.3. (If it were not true, then a localized wave packet, which propagates at the group velocity, would move along a different trajectory from its energy, and we would wind up with energy in regions with vanishing amplitude!)

20.3.4 Langmuir Waves and Ion Acoustic Waves in Warm Plasmas

For our case of a cold, unmagnetized plasma, the third pair of modes embodied in the dispersion relation (20.21) only exists at a single frequency, the plasma frequency $\omega = \omega_p$. These modes' wave equation $L_{ij}E_j = 0$ with $||L_{ij}|| = \mathrm{diag}(-k^2, -k^2, 0)$ [Eq. (20.20) with $\omega^2 = \omega_p^2$] implies that $\mathbf{E}$ points in the z-direction, i.e., along $\mathbf{k}$; the Maxwell equations then imply $\mathbf{B} = 0$, and the equations of motion (20.15) imply that the fluid displacements are in the direction of $\mathbf{E}$. Clearly, these modes, like electromagnetic modes in the limit $k = 0$ and $\omega = \omega_p$, are electrostatic plasma oscillations. However, in this case where the spatial variations of $\mathbf{E}$ and $\mathbf{u}_s$ are along the direction of oscillation instead of perpendicular, k is not constrained to vanish; rather, all wave numbers are allowed. This means that the plasma can undergo plane-parallel oscillations at $\omega = \omega_p$ with displacements in some Cartesian z-direction, and any arbitrary z-dependent amplitude that one might wish. But these oscillations cannot transport energy; because ω is independent of $\mathbf{k}$, their group velocity $\mathbf{V}_g = \nabla_{\mathbf{k}}\omega$ vanishes.

So far we have confined ourselves to wave modes in cold plasmas and have ignored thermal motions of the particles. When thermal motions are turned on, the resulting thermal pressure

gradients convert longitudinal plasma oscillations, at finite wave number k, into propagating, energy-transporting modes called *Langmuir waves*. As we have already intimated, because the plasma is collisionless, to understand the thermal effects fully we must turn to kinetic theory (Chap. 21). However, within the present chapter's two-fluid formalism, we can deduce the leading order effects of finite temperature with the guidance of physical arguments:

The key to the Langumir waves' propagation is the warm electrons' thermal pressure. (The proton pressure is unimportant because the protons oscillate electrostically with an amplitude that is tiny compared to the electrons.) Now, in an adiabatic sound wave in a fluid (where the particle mean free paths are small compared to the wavelength), we relate the pressure perturbation to the density perturbation by assuming that the entropy is constant. In other words, we write $\boldsymbol{\nabla} P = c_s^2 m \boldsymbol{\nabla} n$, where $c_s = (\gamma P/nm)^{1/2}$ is the adiabatic sound speed, n is the particle density, m the particle mass, and γ is the specific heat ratio, which is $5/3$ for a monatomic gas. However, the electron gas is collisionless and we are only interested in the tensorial pressure gradient parallel to $\mathbf{k}$ (which we take to point in the z direction), $\delta P_{e\,zz,z}$. We can therefore ignore all electron motion perpendicular to the wave vector as this is not coupled to the parallel motion. (This would not be a valid assumption if a strong magnetic field were present.) The electron motion is then effectively one dimensional as there is only one (translational) degree of freedom. The relevant specific heat at constant volume is therefore just $k_B/2$ per electron, while that at constant pressure is $3k_B/2$, giving $\gamma = 3$. The effective sound speed for the electron gas is then $c_s = (3k_B T_e/m_e)^{1/2}$, and correspondingly the perturbations of longitudinal electron pressure and electron density are related by

$$\frac{\delta P_{e\,zz}}{m_e \delta n_e} = c_s^2 = \frac{3k_B T_e}{m_e} \ . \tag{20.30}$$

This is one of the equations governing Langmuir waves. The others are the linearized equation of continuity (20.13) which relates the electrons' density perturbation to the longitudinal component of their fluid velocity perturbation

$$\delta n_e = n_e \frac{k}{\omega} u_{e\,z} \ , \tag{20.31}$$

the linearized equation of motion (20.14) which relates $u_{e\,z}$ and $\delta P_{e\,zz}$ to the longitudinal component of the oscillating electric field

$$-i\omega n_e m_e u_{e\,z} = ik \delta P_{e\,zz} - n_e e E_z \ , \tag{20.32}$$

and the linearized form of Poisson's equation $\boldsymbol{\nabla} \cdot \mathbf{E} = \rho_e/\epsilon_0$ which relates E_z to δn_e

$$ikE_z = -\frac{\delta n_e e}{\epsilon_0} \ . \tag{20.33}$$

Equations (20.30)–(20.33) are four equations for three ratios of the perturbed quantities. By combining these equations, we obtain a condition that must be satisfied in order for them to have a solution:

$$\boxed{\omega^2 = \omega_{pe}^2 + \frac{3k_B T_e}{m_e} k^2 = \omega_{pe}^2 (1 + 3k^2 \lambda_D^2) \ ;} \tag{20.34}$$

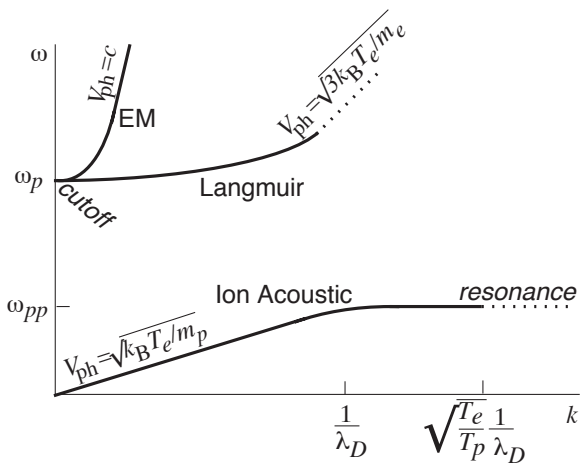

Fig. 20.1: Dispersion relations for electromagnetic waves, Langmuir waves, and ion-acoustic waves in an unmagnetized plasma. In the dotted regions the waves are strongly damped, according to kinetic-theory analyses in Chap. 21.

here $\lambda_D = \sqrt{\epsilon_0 k_B T_e / n_e e^2}$ is the Debye length [Eq. (18.10)]. Equation (20.34) is the *Bohm-Gross* dispersion relation for Langmuir waves.

From this dispersion relation we deduce the phase speed of a Langmuir wave:

$$V_{\rm ph} = \left(\frac{k_B T_e}{m_e}\right)^{1/2} \left(3 + \frac{1}{k^2 \lambda_D^2}\right)^{1/2} . \tag{20.35}$$

Evidently, when the wavelength is less than or of order the Debye length ($k\lambda_D \gtrsim 1$), the phase speed becomes comparable with the electron thermal speed. It is then possible for individual electrons to transfer energy between adjacent compressions and rarefactions in the wave. As we shall see in the next chapter, when we recover Eq. (20.34) from a kinetic treatment, the resulting energy transfers damp the wave. Therefore, the Bohm-Gross dispersion relation is only valid for wavelengths much longer than the Debye length, i.e. $k\lambda_D \ll 1$; cf. Fig. 20.1.

In our analysis of Langmuir waves, we have ignored the proton motion. This is justified as long as the proton thermal speeds are small compared to the electron thermal speeds, i.e. $T_p \ll m_p T_e/m_e$, which will almost always be the case. Proton motion is, however, not ignorable in a second type of plasma waves that owe its existence to finite temperature: *ion acoustic waves*. These are waves that propagate with frequencies far below the electron plasma frequency—frequencies so low that the electrons remain locked electrostatically to the protons, keeping the plasma charge neutral and preventing electromagnetic fields from participating in the oscillations. As for Langmuir waves, we can derive the ion-acoustic dispersion relation using fluid theory combined with physical arguments:

In the next chapter, using kinetic theory we shall see that ion acoustic waves can propagate only when the proton temperature is very small compared with the electron temperature, $T_p \ll T_e$; otherwise they are damped. (Such a temperature disparity is produced, e.g., when a plasma passes through a shock wave, and it can be maintained for a long time because Coulomb collisions are so ineffective at restoring $T_p \sim T_e$; cf. Sec. 18.4.3.) Because $T_p \ll T_e$,

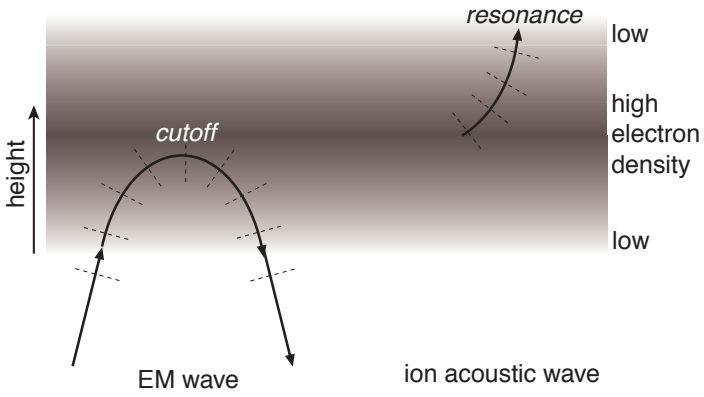

Fig. 20.2: Cutoff and resonance illustrated by wave propagation in the Earth's ionosphere. The thick, arrowed curves are rays and the thin, dashed curves are phase fronts. The electron density is proportional to the darkness of the shading.

the proton pressure can be ignored and the waves' restoring force is provided by electron pressure. Now, in an ion acoustic wave, by contrast with a Langmuir wave, the individual thermal electrons can travel over many wave lengths during a single wave period, so the electrons remain isothermal as their mean motion oscillates in lock-step with the protons' mean motion. Correspondingly, the electrons' effective (one-dimensional) specific heat ratio is $\gamma_{\rm eff} = 1$.

Although the electrons provide the ion-acoustic waves' restoring force, the inertia of the electrostatically-locked electrons and protons is almost entirely that of the heavy protons. Correspondingly, the waves' phase velocity is

$$\mathbf{V}_{ia} = \left(\frac{\gamma_{\rm eff} P_e}{n_p m_p}\right)^{1/2} \hat{k} = \left(\frac{k_B T_e}{m_p}\right)^{1/2} \hat{k} \ , \tag{20.36}$$

[cf. Ex. 20.4] and the dispersion relation is $\omega = V_{\rm ph} k = (k_B T_e/m_p)^{1/2} k$.

From this phase velocity and our physical description of these ion-acoustic waves, it should be evident that they are the magnetosonic waves of MHD theory (Sec. 17.7.2), in the limit that the plasma's magnetic field is turned off.

In Ex. 20.4, we show that the character of these waves gets modified when their wavelength becomes of order the Debye length, i.e. when $k\lambda_D \sim 1$. The dispersion relation then gets modified to

$$\boxed{\omega = \left(\frac{k_B T_e/m_p}{1+\lambda_D^2 k^2}\right)^{1/2} k \ ,} \tag{20.37}$$

which means that for $k\lambda_D \gg 1$, the waves' frequency approaches the *proton plasma frequency* $\omega_{pp} \equiv \sqrt{ne^2/\epsilon_0 m_p} \simeq \sqrt{m_e/m_p}\omega_p$. A kinetic-theory treatment reveals that these waves are strong damped when $k\lambda_D \gtrsim \sqrt{T_e/T_p}$. These features of the ion-acoustic dispersion relation are illustrated in Fig. 20.1.

20.3.5 Cutoffs and Resonances

Electomagnetic waves, Langmuir waves and ion-acoustic waves in an unmagnetized plasma provide examples of *cutoffs* and *resonances*.

A *cutoff* is a frequency at which a wave mode ceases to propagate, because its wave number k there becomes zero. Langmuir and electromagnetic waves at $\omega \to \omega_p$ are examples; see Fig. 20.1. Consider, for concreteness, a monochromatic radio-frequency electromagnetic wave propagating upward into the earth's ionosphere at some nonzero angle to the vertical (left side of Fig. 20.2), and neglect the effects of the earth's magnetic field. As the wave moves deeper (higher) into the ionosphere, it encounters a rising electron density n and correspondingly a rising plasma frequency ω_p. The wave's wavelength will typically be small compared to the inhomogeneity scale for ω_p, so the wave propagation can be analyzed using geometric optics (Sec. 6.3). Across a phase front, that portion which is higher in the ionosphere will have a smaller k and thus a larger wavelength and phase speed, and thus a greater distance between phase fronts (dashed lines). Therefore, the rays, which are orthogonal to the phase fronts, will bend away from the vertical (left side of Fig. 20.2); i.e., the wave will be reflected away from the cutoff at which $\omega_p \to \omega$ and $k \to 0$. Clearly, this behavior is quite general. Wave modes are generally reflected from regions in which slowly changing plasma conditions give rise to cutoffs.

A *resonance* is a frequency at which a wave mode ceases to propagate because its wave number k there becomes infinite, i.e. its wavelength goes to zero. Ion-acoustic waves provide an example; see Fig. 20.1. Consider, for concreteness, an ion-acoustic wave deep within the ionosphere, where ω_{pp} is larger than the wave's frequency ω. As the wave propagates toward the upper edge of the ionosphere, at some nonzero angle to the vertical, the portion of a phase front that is higher sees a smaller electron density and thus a smaller ω_{pp}, and thence has a larger k and shorter wavelength, and thus a shorter distance between phase fronts (dashed lines). This causes the rays to bend toward the vertical (right side of Fig. 20.2). The wave is "attracted" into the region of the resonance, $\omega \to \omega_{pp}$, $k \to \infty$, where it gets "Landau damped" (Chap. 21) and dies. This behavior is quite general. Wave modes are generally attracted toward regions in which slowly changing plasma conditions give rise to resonances, and upon reaching a resonance, they die.

We shall study wave propagation in the ionosphere in greater detail in Sec. 20.5 below.

****

EXERCISES

Exercise 20.1 *Derivation: Time-averaged energy density in a wave mode*
Verify Eq. (20.27).

Exercise 20.2 *Example: Effect of Collisional Damping*
Consider a transverse electromagnetic wave mode propagating in an unmagnetized, partially ionized gas in which the electron-neutral collision frequency is ν_e. Include the effects of collisions in the electron equation of motion, Eq. (20.15), by introducing a term $-n_e m_e \nu_e \mathbf{u}_e$ on the right hand side. Ignore ion motion and electron-ion and electron-electron collisions.

Derive the dispersion relation when $\omega \gg \nu_e$ and show by explicit calculation that the rate of loss of energy per unit volume ($-\boldsymbol{\nabla}\cdot\mathbf{S}$, where $\mathbf{S}$ is the Poynting flux) is balanced by the Ohmic heating of the plasma. (Hint: It may be easiest to regard ω as real and $\mathbf{k}$ as complex.)

Exercise 20.3 *Problem: Fluid Drifts in a Time-Independent Plasma*
Consider a hydrogen plasma described by the two-fluid formalism. Suppose that Coulomb collisions have had time to isotropize the electrons and protons and to equalize their temperatures so that their partial pressures $P_e = n_e k_B T$ and $P_p = n_p k_B T$ are equal. An electric field $\mathbf{E}$ created by external charges is applied.

(a) Using the law of force balance for fluid s, show that its drift velocity perpendicular to the magnetic field is

$$v_{s\perp} = \frac{\mathbf{E}\times\mathbf{B}}{B^2} - \frac{\boldsymbol{\nabla}P_s\times\mathbf{B}}{q_s n_s B^2} - \frac{m_s}{q_s B^2}[(\mathbf{v}_s\cdot\boldsymbol{\nabla})\mathbf{v}_s]_\perp\times\mathbf{B}\ . \tag{20.38}$$

The first term is the $\mathbf{E}\times\mathbf{B}$ drift discussed in Chap. 19.

(b) The second term, called the "diamagnetic drift," is different for the electrons and the protons. Show that this drift produces a current density perpendicular to $\mathbf{B}$ given by

$$\mathbf{j}_\perp = \frac{(\boldsymbol{\nabla}P)\times\mathbf{B}}{B^2}\ , \tag{20.39}$$

where P is the total pressure.

(c) The third term can be called the "drift-induced drift". Show that if the electrons are nearly locked to the ion motion, then the associated current density is well approximated by

$$\mathbf{j}_\perp = -\frac{\rho}{B^2}[(\mathbf{v}\cdot\boldsymbol{\nabla})\mathbf{v}]\times\mathbf{B}\ , \tag{20.40}$$

where ρ is the density and $\mathbf{v}$ is the average fluid speed. These results are equivalent to those obtained using a pure MHD treatment.

Exercise 20.4 *Derivation: Ion Acoustic Waves*
Ion acoustic waves can propagate in an unmagnetized plasma when the electron temperature T_e greatly exceeds the ion temperature. In this limit the electron density n_e can be approximated by $n_e = n_0\exp(e\Phi/k_B T_e)$, where n_0 is the mean electron density and Φ is the electrostatic potential.

(a) Show that the nonlinear equations of continuity and motion for the ion (proton) fluid and Poisson's equation for the potential take the form

$$\begin{aligned}
\frac{\partial n}{\partial t} + \frac{\partial(nu)}{\partial z} &= 0\ ,\\
\frac{\partial u}{\partial t} + u\frac{\partial u}{\partial z} &= -\frac{e}{m_p}\frac{\partial\Phi}{\partial z}\ ,\\
\frac{\partial^2\Phi}{\partial z^2} &= -\frac{e}{\epsilon_0}(n - n_0 e^{e\Phi/k_B T_e})\ ,
\end{aligned} \tag{20.41}$$

where n is the proton density, u is the proton fluid velocity, and the waves propagate in the z direction.

(b) Linearize these equations and show that the dispersion relation for small-amplitude ion acoustic modes is

$$\omega = \omega_{pp}\left(1+\frac{1}{\lambda_D^2 k^2}\right)^{-1/2} = \left(\frac{k_B T_e/m_p}{1+\lambda_D^2 k^2}\right)^{1/2} k \ , \tag{20.42}$$

where λ_D is the Debye length. Verify that in the long-wavelength limit, this agrees with Eq. (20.36).

Exercise 20.5 *Challenge: Ion Acoustic Solitons*
In this exercise we shall explore nonlinear effects in ion acoustic waves (Ex. 20.4), and shall show that they give rise to solitons that obey the same Korteweg-de Vries equation as governs solitonic water waves (Sec. 15.3).

(a) Introduce an expansion parameter $\varepsilon \ll 1$ and expand the ion density, ion velocity and potential in the form

$$\begin{aligned} n &= n_0(1+\varepsilon n_1+\varepsilon^2 n_2+\dots) \ , \\ u &= (k_B T_e/m_p)^{1/2}(\varepsilon u_1+\varepsilon^2 u_2+\dots) \ , \\ \Phi &= (k_B T_e/e)(\varepsilon\Phi_1+\varepsilon^2\Phi_2+\dots) \ . \end{aligned} \tag{20.43}$$

Change independent variables from (t,z) to (τ,η) where

$$\begin{aligned} \eta &= \sqrt{2}\varepsilon^{1/2}\lambda_D^{-1}[z-(k_B T_e/m_p)^{1/2}t] \ , \\ \tau &= \sqrt{2}\varepsilon^{3/2}\omega_{pp}t \ . \end{aligned} \tag{20.44}$$

By substituting Eqs. (20.43) and (20.44) into the nonlinear equations (20.41) and equating terms of the same order, show that n_1, u_1, Φ_1 *each* satisfy the Korteweg-de Vries equation (15.32):

$$\frac{\partial\zeta}{\partial\tau}+\zeta\frac{\partial\zeta}{\partial\eta}+\frac{\partial^3\zeta}{\partial\eta^3}=0 \ . \tag{20.45}$$

(b) In Sec. 15.3 we discussed the exact, single-soliton solution (15.33) to this KdV equation. Show that for an ion-acoustic soliton, this solution propagates with the physical speed $(1+\varepsilon)(k_B T_e/m_p)^{1/2}$, which is greater the larger is the wave's amplitude ε.

****

20.4 Wave Modes in a Cold, Magnetized Plasma

20.4.1 Dielectric Tensor and Dispersion Relation

We now complicate matters somewhat by introducing a uniform magnetic field $\mathbf{B}_0$ into the unperturbed plasma. To avoid further complications, we make the plasma cold, i.e. we omit thermal effects. The linearized equation of motion for each species then becomes

$$-i\omega\mathbf{u}_s = \frac{q_s\mathbf{E}}{m_s} + \frac{q_s}{m_s}\mathbf{u}_s \times \mathbf{B}_0 \ . \tag{20.46}$$

It is convenient to multiply this equation of motion by $n_s q_s/\epsilon_0$ and introduce a scalar plasma frequency and scalar and vectorial cyclotron frequencies for each species

$$\boxed{\omega_{ps} = \left(\frac{n_s q_s^2}{\epsilon_0 m_s}\right)^{1/2} \ , \quad \omega_{cs} = \frac{q_s B_0}{m_s} \ , \quad \boldsymbol{\omega}_{cs} = \omega_{cs}\hat{\mathbf{B}}_0 = \frac{q_s\mathbf{B}_0}{m_s}} \tag{20.47}$$

[so $\omega_{pp} = \sqrt{(m_e/m_p)}\,\omega_{pe} \simeq \omega_{pe}/43$, $\omega_{ce} < 0$, $\omega_{cp} > 0$, and $\omega_{cp} = (m_e/m_p)|\omega_{ce}| \simeq |\omega_{ce}|/1860$]. Thereby we bring the equation of motion into the form

$$-i\omega\left(\frac{nq_s}{\epsilon_0}\mathbf{u}_s\right) + \boldsymbol{\omega}_{cs} \times \left(\frac{nq_s}{\epsilon_0}\mathbf{u}_s\right) = \omega_{ps}^2\mathbf{E} \ . \tag{20.48}$$

By combining this equation with $\boldsymbol{\omega}_{cs}\times$(this equation), we can solve for the fluid velocity of species s as a linear function of the electric field $\mathbf{E}$:

$$\boxed{\frac{n_s q_s}{\epsilon_0}\mathbf{u}_s = -i\left(\frac{\omega\omega_{ps}^2}{\omega_{cs}^2 - \omega^2}\right)\mathbf{E} - \frac{\omega_{ps}^2}{(\omega_{cs}^2 - \omega^2)}\boldsymbol{\omega}_{cs} \times \mathbf{E} + \boldsymbol{\omega}_{cs}\frac{i\omega_{ps}^2}{(\omega_{cs}^2 - \omega^2)\omega}\boldsymbol{\omega}_{cs} \cdot \mathbf{E} \ .} \tag{20.49}$$

(This relation is useful when one tries to deduce the physical properties of a wave mode.) From this fluid velocity we can read off the current $\mathbf{j} = \sum_s n_s q_s \mathbf{u}_s$ as a linear function of $\mathbf{E}$; by comparing with Ohm's law $\mathbf{j} = \boldsymbol{\kappa}_{\rm e} \cdot \mathbf{E}$, we then obtain the tensorial conductivity $\boldsymbol{\kappa}_{\rm e}$, which we insert into Eq. (20.18) to get the following expression for the dielectric tensor (in which $\mathbf{B}_0$ and thence $\boldsymbol{\omega}_{cs}$ is taken to be along the z axis):

$$\boldsymbol{\epsilon} = \begin{pmatrix} \epsilon_1 & -i\epsilon_2 & 0 \\ i\epsilon_2 & \epsilon_1 & 0 \\ 0 & 0 & \epsilon_3 \end{pmatrix} \ , \tag{20.50}$$

where

$$\boxed{\epsilon_1 = 1 - \sum_s \frac{\omega_{ps}^2}{\omega^2 - \omega_{cs}^2} \ , \quad \epsilon_2 = \sum_s \frac{\omega_{ps}^2\omega_{cs}}{\omega(\omega^2 - \omega_{cs}^2)} \ , \quad \epsilon_3 = 1 - \sum_s \frac{\omega_{ps}^2}{\omega^2} \ .} \tag{20.51}$$

Let the wave propagate in the x–z plane, at an angle θ to the z-axis (i.e. to the magnetic field). Then the algebratized wave operator (20.8) takes the form

$$||L_{ij}|| = \frac{\omega^2}{c^2}\begin{pmatrix} \epsilon_1 - \tilde{n}^2\cos^2\theta & -i\epsilon_2 & \tilde{n}^2\sin\theta\cos\theta \\ i\epsilon_2 & \epsilon_1 - \tilde{n}^2 & 0 \\ \tilde{n}^2\sin\theta\cos\theta & 0 & \epsilon_3 - \tilde{n}^2\sin^2\theta \end{pmatrix} \ , \tag{20.52}$$

where

$$\boxed{\tilde{n} = \frac{ck}{\omega}} \tag{20.53}$$

is the wave's index of refraction—i.e, the wave's phase velocity is $V_{\rm ph} = \omega/k = c/\tilde{n}$. (We introduce the tilde in this chapter to distinguish $\tilde{n}$ from the particle density n.) The algebratized wave operator (20.52) will be needed when we explore the physical nature of modes, in particular the directions of their electric fields which satisfy $L_{ij}E_j = 0$.

From the wave operator (20.52) we deduce the waves' dispersion relation $\det||L_{ij}|| = 0$. Some algebra brings this into the form

$$\boxed{\tan^2\theta = \frac{-\epsilon_3(\tilde{n}^2 - \epsilon_R)(\tilde{n}^2 - \epsilon_L)}{\epsilon_1(\tilde{n}^2 - \epsilon_3)\left(\tilde{n}^2 - \frac{\epsilon_R\epsilon_L}{\epsilon_1}\right)}} , \tag{20.54}$$

where

$$\boxed{\epsilon_L = \epsilon_1 - \epsilon_2 = 1 - \sum_s \frac{\omega_{ps}^2}{\omega(\omega - \omega_{cs})} , \quad \epsilon_R = \epsilon_1 + \epsilon_2 = 1 - \sum_s \frac{\omega_{ps}^2}{\omega(\omega + \omega_{cs})} .} \tag{20.55}$$

20.4.2 Parallel Propagation

As a first step in making sense out of the general dispersion relation (20.54) for waves in a cold, magnetized plasma, let us consider wave propagation along the magnetic field, so $\theta = 0$. The dispersion relation (20.54) then factorizes to give three pairs of solutions:

$$\begin{aligned} \frac{c^2k^2}{\omega^2} &= \epsilon_L , \\ \frac{c^2k^2}{\omega^2} &= \epsilon_R , \\ \epsilon_3 &= 0 . \end{aligned} \tag{20.56}$$

Consider the first solution (20.56), $\tilde{n}^2 = \epsilon_L$. The algebratized wave equation $L_{ij}E_j = 0$ in this case requires that the electric field direction be $\mathbf{E} \propto (\mathbf{e}_x - i\mathbf{e}_y)e^{-i\omega t}$, which is a left-hand circularly polarized wave propagating along the static magnetic field (z direction). The second solution (20.56), $\tilde{n}^2 = \epsilon_R$, is the corresponding right-hand circular polarized mode. From Eqs. (20.55) we see that these two modes propagate with different phase velocities (but only slightly different, if ω is far from the electron cyclotron frequency and far from the proton cyclotron frequency.) The third solution (20.56), $\epsilon_3 = 0$, is just the electrostatic plasma oscillation in which the electrons and protons oscillate parallel to and are unaffected by the static magnetic field.

As an aid to exploring the frequency dependence of the left and right modes, we plot in Fig. 20.3 the refractive index $n = ck/\omega$ as a function of $\omega/|\omega_{ce}|$.

In the high-frequency limit, the refractive index for both modes is slightly less than unity and approaches that for an unmagnetized plasma, $\tilde{n} = ck/\omega \simeq 1 - \frac{1}{2}\omega_p^2/\omega^2$ [cf. Eq. (20.25)],

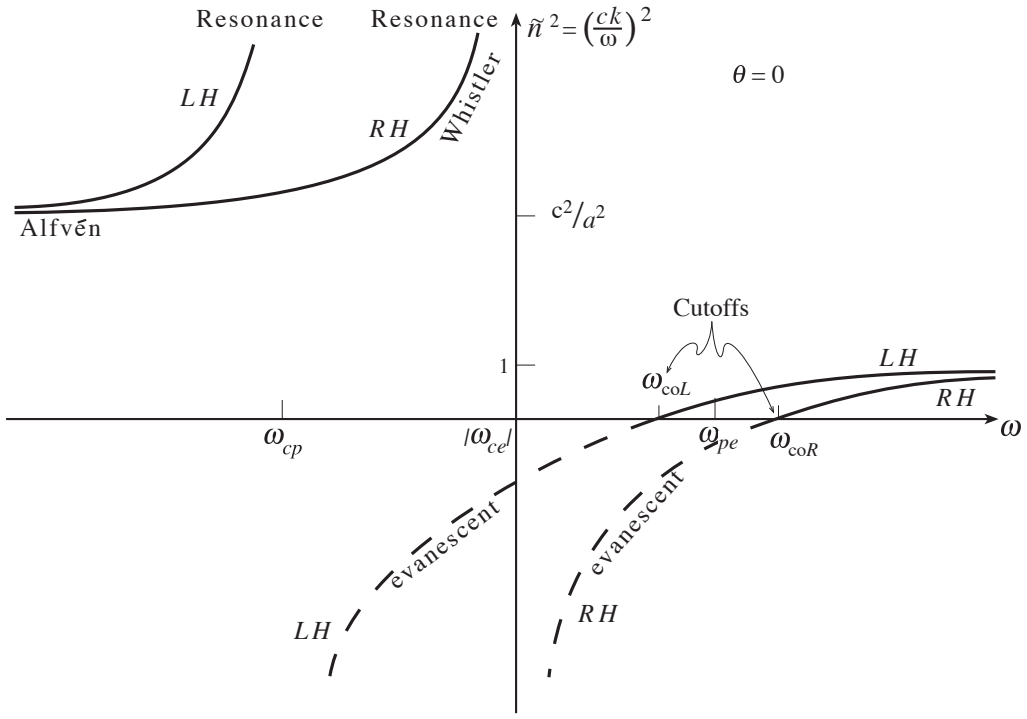

Fig. 20.3: Square of wave refractive index for circularly polarized waves propagating along the static magnetic field in a proton-electron plasma with $\omega_{pe} > \omega_{ce}$. (Remember, that we will regard both the electron and the proton cyclotron frequencies as positive numbers.) The angular frequency is plotted logarithmically in units of the modulus of the electron gyro frequency.

but with a small difference between the modes given to leading order by

$$\tilde{n}_L - \tilde{n}_R \simeq \frac{\omega_{pe}^2 \omega_{ce}}{\omega^3} \tag{20.57}$$

This difference is responsible for an important effect known as *Faraday rotation*:

Suppose that a linearly polarized wave is incident upon a magnetized plasma and propagates parallel to the magnetic field. We can deduce the behavior of the polarization by expanding the mode as a linear superposition of the two circular polarized eigenmodes, left and right. These two modes propagate with slightly different phase velocities, so after propagating some distance through the plasma, they acquire a relative phase shift $\delta\phi$. When one then reconstitutes the linear polarized mode from the circular eigenmodes, this phase shift is manifest in a rotation of the plane of polarisation through an angle $\Delta\phi/2$ (for small $\Delta\phi$). This, together with the difference in refractive indices (20.57) (which determines $\Delta\phi$) implies a rotation rate for the plane of polarization given by

$$\frac{d\chi}{dz} = \frac{\omega_{pe}^2 \omega_{ce}}{2\omega^2 c} \ . \tag{20.58}$$

As the wave frequency is reduced, the refractive index decreases to zero, first for the right circular wave, then for the left circular wave; cf. Fig. 20.3. Vanishing at a finite frequency

corresponds to vanishing of k and infinite wavelength, i.e., it signals a *cutoff*; cf. Fig. 20.2 and associated discussion. When the frequency is lowered further, the refractive index becomes negative and the wave mode becomes evanescent. In other words, if we imagine a wave of constant frequency propagating into an inhomogeneous plasma parallel to its density gradient then solving the dispersion relation (20.22) for k we find that purely imaginary values for k are required if $\omega < \omega_{\rm cutoff}$.

The cutoff frequencies are different for the two modes and are given by

$$\begin{aligned}\omega_{{\rm co}R,L} &= \frac{1}{2}\left[\left\{(\omega_{ce}+\omega_{cp})^2 + 4(\omega_{pe}^2+\omega_{pp}^2)\right\}^{1/2} \pm (|\omega_{ce}| - \omega_{cp})\right] \\ &\simeq \omega_{pe} \pm |\omega_{ce}| \end{aligned} \tag{20.59}$$

assuming (as us usually the case) that $\omega_{pe} \gg |\omega_{ce}|$.

As we lower the frequency further (Fig. 20.3), first the right mode and then the left regain the ability to propagate. When the wave frequency lies between the proton and electron gyro freqencies, $\omega_{cp} < \omega < |\omega_{ce}|$, only the right mode propagates. This mode is sometimes called a *whistler*. As its frequency increases toward the electron gyro frequency $|\omega_{ce}|$ (where it first recovered the ability to propagate), its refractive index and wave vector become infinite—a signal that $\omega = |\omega_{ce}|$ is a *resonance* for the whistler; cf. Fig. 20.2. The physical origin of this resonance is that the wave frequency becomes resonant with the gyrational frequency of the electrons that are orbiting the magnetic field in the same sense as the wave's electric vector rotates. To quantify the strong wave absorption that occurs at this resonance, one must carry out a kinetic-theory analysis that takes account of the electrons' thermal motions (Chap. 21).

Another feature of the whistler is that it is highly dispersive close to resonance; its dispersion relation there is given approximately by

$$\omega \simeq \frac{|\omega_{ce}|}{1+\omega_{pe}^2/c^2k^2} \tag{20.60}$$

The group velocity, obtained by differentiating Eq. (20.60), is given approximately by

$$\mathbf{V}_g = \left|\frac{\partial\omega}{\partial\mathbf{k}}\right| \simeq \frac{2\omega_{ce}c}{\omega_{pe}}\left(1-\frac{\omega}{|\omega_{ce}|}\right)^{3/2}\hat{\mathbf{B}}_0\ . \tag{20.61}$$

This velocity varies extremely rapidly close to resonance, so waves of different frequency propagate at very different speeds.

This is the physical origin of the phenomenon by which whistlers were discovered, historically. They were first encountered by radio operators who heard strange tones with rapidly changing pitch in their earphones. These turned out to be whistler modes excited by lightning in the southern hemisphere that propagated along the earth's magnetic field through the magnetosphere to the northern hemisphere. Only modes below the lowest electron gyro frequency on the path could propagate and these were highly dispersed, with the lower frequencies arriving first.

There is also a resonance associated with the right hand polarized wave, which propagates below the proton cyclotron frequency; see Fig. 20.3.

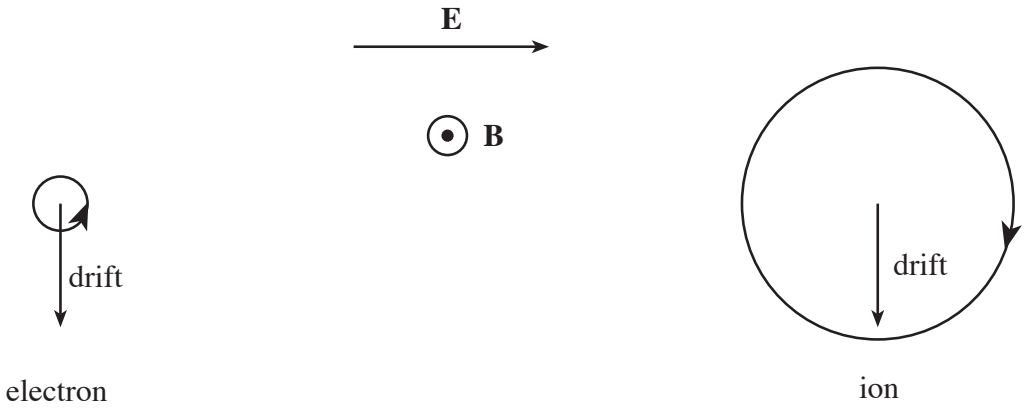

Fig. 20.4: Gyration of electrons and ions in a low frequency Alfvén wave. Although the electrons and ions gyrate with opposite senses about the magnetic field, their $\mathbf{E} \times \mathbf{B}$ drifts are similar. It is only in the next highest order of approximation that a net ion current is produced parallel to the applied electric field.

Finally, let us examine the low frequency limit of these waves (Fig. 20.3). We find that for both modes,

$$\omega = ak\left(1 + \frac{a^2}{c^2}\right)^{-1/2} , \tag{20.62}$$

where $a = B_0\{\mu_0 n_e(m_p + m_e)\}^{-1/2}$ is the Alfvén speed that arose in our discussion of magnetohydrodynamics [Eq. (17.76)]. As this chapter's two-fluid physical description is more detailed than the MHD treatment, it is not surprising that the degeneracy between the two propagating modes that exists in MHD is broken and we find that there are two circular polarized eigenmodes travelling with slightly different speeds.

The phase speed $a/\sqrt{1 + a^2/c^2}$ to which both modes asymptote, as $\omega \to 0$, is slightly lower than the Alfvén speed. This fact could not be deduced using nonrelativistic MHD, because it neglects the displacement current.

It is illuminating to consider what is happening to the particles in a very-low-frequency Alfvén wave; see Fig. 20.4. As the wave frequency is below both the electron and the proton cyclotron frequencies, both types of particle will orbit the $\mathbf{B}_0$ field many times in a wave period. When the wave electric field is applied, the guiding centers of both types of orbits undergo the same $\mathbf{E} \times \mathbf{B}$ drift, so the two fluid velocities also drift at this rate and the currents associated with the proton and electron drifts cancel. However, when we consider higher-order corrections to the guiding center response, we find that the ions drift slightly faster than the electrons, which produces a net current that modifies the magnetic field and gives rise to the modified propagation speed.

20.4.3 Perpendicular Propagation

Turn, next, to waves that propagate perpendicular to the static magnetic field, ($\mathbf{k} = k\mathbf{e}_x$; $\theta = \pi/2$). In this case our general dispersion relation (20.54) again has three solutions

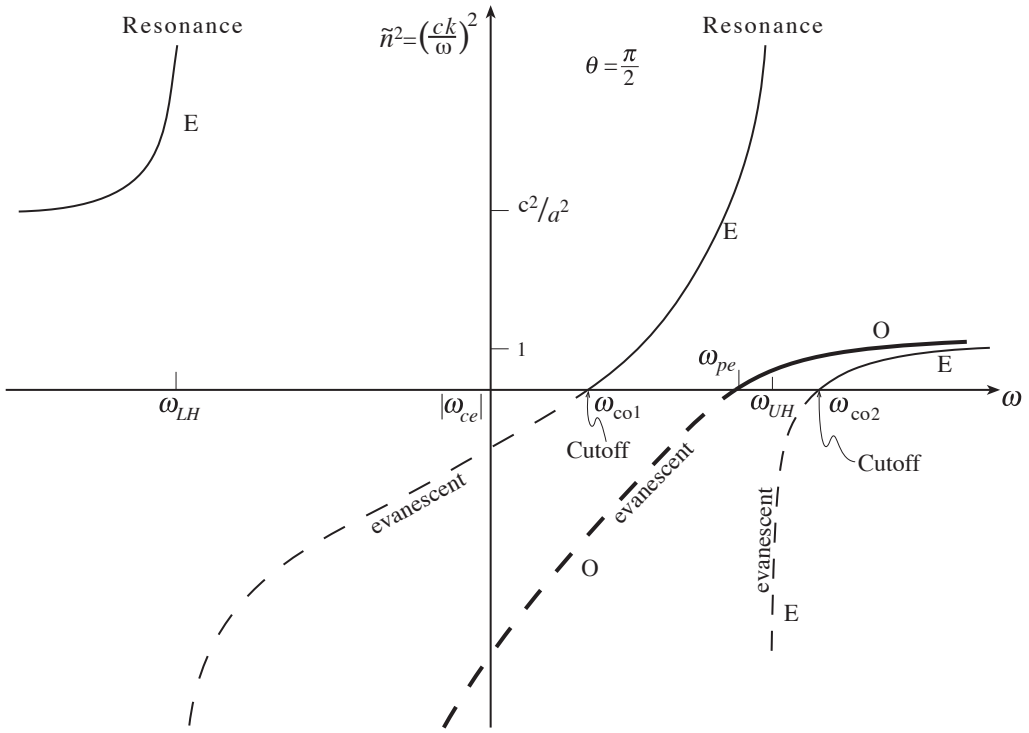

Fig. 20.5: Variation of refractive index $\tilde{n}$ for wave propagation perpendicular to the magnetic field in an electron ion plasma with $\omega_{pe} > \omega_{ce}$. The ordinary mode is designated by O, the extraordinary mode by E.

corresponding to three modes:

$$\begin{aligned} \frac{c^2k^2}{\omega^2} &= \epsilon_3 \ , \\ \frac{c^2k^2}{\omega^2} &= \frac{\epsilon_R\epsilon_L}{\epsilon_1} \ , \\ \epsilon_1 &= 0 \ . \end{aligned} \tag{20.63}$$

The first solution

$$\tilde{n}^2 = \epsilon_3 = 1 - \frac{\omega_p^2}{\omega^2} \tag{20.64}$$

has the same index of refraction as for electromagnetic waves in an unmagnetized plasma; cf. Eq. (20.22), so this is called the *ordinary mode*. In this mode, the electric vector and velocity perturbation are parallel to the static magnetic field and so the current response is uninfluenced by it.

The second solution (20.63),

$$\tilde{n}^2 = \epsilon_R\epsilon_L/\epsilon_1 = \frac{\epsilon_1^2 - \epsilon_2^2}{\epsilon_1} \ , \tag{20.65}$$

is known as the *extraordinary mode* and has an electric field that is orthogonal to $\mathbf{B}_0$ but not to $\mathbf{k}$.

The refractive indices for the ordinary and extraordinary modes are plotted as functions of frequency in Fig. 20.5. The ordinary-mode curve is dull; it is just like that in an unmagnetized plasma. The extraordinary-mode curve is more interesting. It has two cutoffs, with frequencies

$$\omega_{co1,2} \simeq \left(\omega_{pe}^2 + \frac{1}{4}\omega_{ce}^2\right)^{1/2} \pm \frac{1}{2}\omega_{ce} \ , \tag{20.66}$$

and two resonances with strong absorption, at frequencies known as the *Upper and Lower Hybrid* frequencies. These frequencies are given approximately by

$$\begin{aligned} \omega_{UH} &\simeq (\omega_{pe}^2 + \omega_{ce}^2)^{1/2} \ , \\ \omega_{LH} &\simeq \left[\frac{(\omega_{pe}^2 + |\omega_{ce}|\omega_{cp})|\omega_{ce}|\omega_{cp}}{\omega_{pe}^2 + \omega_{ce}^2}\right]^{1/2} \ . \end{aligned} \tag{20.67}$$

In the limit of very low frequency, the extraordinary, perpendicularly propagating mode has the same dispersion relation $\omega = ak/\sqrt{1 + a^2/c^2}$ as the paralleling propagating modes [Eq. (20.62)]. It has become the fast magnetosonic wave, propagating perpendicular to the static magnetic field [Sec. 17.7.2], while the parallel waves became the Alfvén modes.

20.5 Propagation of Radio Waves in the Ionosphere

The discovery that radio waves could be reflected off the ionosphere and thereby transmitted over long distances revolutionized communications and stimulated intensive research on radio wave propagation in a magnetoactive plasma. The ionosphere is a dense layer of partially ionized gas between 50 and 300 km above the surface of the earth. The ionization is due to incident solar UV radiation and although the ionization fraction increases with height, the actual density of free electrons passes through a maximum whose height rises and falls with the sun.

The electron gyro frequency varies from ~ 0.5 to ~ 1 MHz over the ionosphere and the plasma frequency increases from effectively zero to a maximum that can be as high as 100 MHz, so typically, $|\omega_{pe}| \gg \omega_{ce}$. We are interested in wave propagation above the electron plasma frequency, which in turn is well in excess of the ion plasma frequency and the ion gyro frequency. It is therefore a good approximation to ignore ion motions altogether. In addition, at the altitudes of most interest for radio wave propagation, the temperature is very low, $T_e \sim 200 - 600$K, and the cold plasma approximation is well motivated. A complication that one must sometimes face in the ionosphere is the influence of collisions (Ex. 20.2 above), but in this section we shall ignore it.

It is conventional in magnetoionic theory to introduce two dimensionless parameters

$$X = \frac{\omega_{pe}^2}{\omega^2} \ , \quad Y = \frac{|\omega_{ce}|}{\omega} \tag{20.68}$$

in terms of which (ignoring ion motions) the components (20.51) of the dielectric tensor are

$$\epsilon_1 = 1 + \frac{X}{Y^2 - 1} , \quad \epsilon_2 = \frac{XY}{Y^2 - 1} , \quad \epsilon_3 = 1 - X . \tag{20.69}$$

It is convenient, in this case, to rewrite the dispersion relation $\det||L_{ij}|| = 0$ in a form different from Eq. (20.54)—a form derivable, e.g., by computing explicitly the determiant of the matrix (20.52), setting

$$x = \frac{X - 1 + \tilde{n}^2}{1 - \tilde{n}^2} , \tag{20.70}$$

solving the resulting quadratic in x, then solving for $\tilde{n}^2$. The result is the *Appleton-Hartree* dispersion relation

$$\tilde{n}^2 = 1 - \frac{X}{1 - \frac{Y^2 \sin^2\theta}{2(1-X)} \pm \left\{ \frac{Y^4 \sin^4\theta}{2(1-X)^2} + Y^2 \cos^2\theta \right\}^{1/2}} \tag{20.71}$$

There are two commonly used approximations to this dispersion relation. The first is the *quasi-longitudinal* approximation, which is used when $\mathbf{k}$ is approximately parallel to the static magnetic field, i.e. when θ is small. In this case, just retaining the dominant terms in the dispersion relation, we obtain

$$\tilde{n}^2 \simeq 1 - \frac{X}{1 \pm Y \cos\theta} . \tag{20.72}$$

This is just the dispersion relation (20.56) for the left and right modes in strictly parallel propagation, with the substitution $B_0 \to B_0 \cos\theta$. By comparing the magnitude of the terms that we dropped from the full dispersion relation in deriving (20.72) with those that we retained, one can show that the quasi-longitudinal approximation is valid when

$$Y^2 \sin^2\theta \ll 2(1 - X)\cos\theta . \tag{20.73}$$

The second approximation is the *quasi-transverse* approximation; it is appropriate when inequality (20.73) is reversed. In this case the two modes are generalizations of the precisely perpendicular ordinary and extraordinary modes, and their approximate dispersion relations are

$$\begin{aligned} \tilde{n}_O^2 &= 1 - X , \\ \tilde{n}_E^2 &= 1 - \frac{X(1-X)}{1 - X - Y^2 \sin^2\theta} . \end{aligned} \tag{20.74}$$

The ordinary-mode dispersion relation is unchanged from the strictly perpendicular one, (20.64); the extraordinary dispersion relation is obtained from the strictly perpendicular one (20.65) by the substitution $B_0 \to B_0 \sin\theta$.

The quasi-longitudinal and quasi-transverse approximations simplify the problem of tracing rays through the ionosphere.

Commercial radio stations operate in the AM (amplitude modulated) (0.5-1.6 MHz), SW (short wave) (2.3-18 MHz) and FM (frequency modulated) (88-108 MHz) bands. Waves in

the first two bands are reflected by the ionosphere and can therefore be transmitted over large surface areas. FM waves, with their higher frequencies, are not reflected and must therefore be received as ground waves. However, they have the advantage of a larger bandwidth and consequently a higher fidelity audio output. As the altitude of the reflecting layer rises at night, short wave communication over long distances becomes easier.

****

EXERCISES

Exercise 20.6 *Example: Dispersion and Faraday rotation of Pulsar pulses*
A radio pulsar emits regular pulses at 1s intervals which propagate to Earth through the ionized interstellar plasma, with electron density $n_e \simeq 3 \times 10^4 \mathrm{m}^{-3}$. The pulses observed at $f = 100$ MHz are believed to be emitted at the same time as those at much higher frequency but arrive with a delay of 100ms.

(a) Explain briefly why pulses travel at the group velocity instead of the phase velocity and show that the expected time delay of the $f = 100$ MHz pulses relative to the high-frequency pulses is given by

$$\Delta t = \frac{e^2}{8\pi^2 m_e \epsilon_0 f^2 c} \int n_e dx \ , \tag{20.75}$$

where the integral is along the waves' propagation path. Hence compute the distance to the pulsar.

(b) Now suppose that the pulses are linearly polarized and that the propagation is accurately described by the quasi-longitudinal approximation. Show that the plane of polarization will be Faraday rotated through an angle

$$\Delta\chi = \frac{e\Delta t}{m_e}\langle B_\parallel \rangle \tag{20.76}$$

where $\langle B_\parallel \rangle = \int n_e \mathbf{B} \cdot d\mathbf{x} / \int n_e dx$. The plane of polarization of the pulses emitted at 100 MHz is believed to be the same as that as at high frequency but is observed to be rotated through 3 radians. Calculate the mean parallel component of the interstellar magnetic field.

Exercise 20.7 *Derivation: Appleton-Hartree Dispersion Relation*
Derive Eq. (20.71)

Exercise 20.8 *Example: Reflection of Short Waves by the Ionosphere*
The free electron density in the night-time ionosphere increases exponentially from $10^9 \mathrm{m}^{-3}$ to $10^{11} \mathrm{m}^{-3}$ as the altitude increases from 100 to 200km and diminishes above this height. Use Snell's law [Eq. (6.43)] to calculate the maximum range of 10 MHz transmission, assuming a single ionospheric reflection.

****

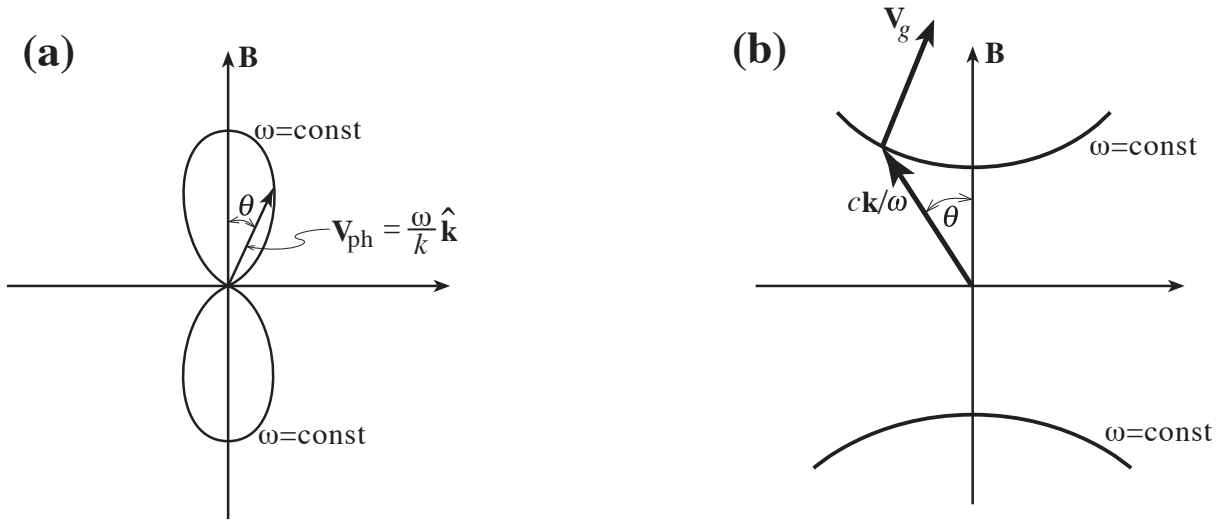

Fig. 20.6: (a) *Wave normal surface* for a whistler mode propagating at an angle θ with respect to the magnetic field direction. In this diagram we plot the phase velocity $\mathbf{V}_{\rm ph} = (\omega/k)\hat{\mathbf{k}}$ as a vector from the origin, with the direction of the magnetic field chosen upward. When we fix the frequency ω of the wave, the tip of the phase velocity vector sweeps out the figure-8 curve as its angle θ to the magnetic field changes. This curve should be thought of as rotated around the vertical (magnetic-field) direction to form a figure-8 "wave-normal" surface. Note that there are some directions where no mode can propagate. (b) *Refractive index surface* for the same whistler mode. Here we plot $c\mathbf{k}/\omega$ as a vector from the origin, and as its direction changes with fixed ω, this vector sweeps out the two hyperboloid-like surfaces. Since the length of the vector is $ck/\omega = \tilde{n}$, this figure can be thought of as a polar plot of the refractive index $\tilde{n}$ as a function of wave propagation direction θ for fixed ω; hence the name "refractive index surface". The group velocity $\mathbf{V}_g$ is orthogonal to the refractive-index surface (Ex. 20.10). Note that for this Whistler mode, the energy flow (along $\mathbf{V}_g$) is focused toward the direction of the magnetic field.

20.6 CMA Diagram for Wave Modes in Cold, Magnetized Plasma

Magnetoactive plasmas are anisotropic, just like optically active crystals. This implies that the phase speed of a propagating wave mode depends upon the angle between the direction of propagation and the magnetic field. There are two convenient ways to exhibit this anisotropy diagramatically. The first method, due originally to Fresnel, is to construct *phase velocity surfaces* (also called *wave-normal surfaces*), which are polar plots of the wave phase velocity $V_{\rm ph} = \omega/k$ as a function of the angle θ that the wave vector $\mathbf{k}$ makes with the magnetic field; see Fig. 20.6(a).

The second type of surface, used originally by Hamilton, is the *refractive index surface*. This is a polar plot of the refractive index $n = ck/\omega$ for a given frequency again as a function of the wave vector's angle θ to $\mathbf{B}$; see Fig. 20.6(b). This has the important property that the group velocity is perpendicular to the surface. As discussed above the energy flow is along the direction of the group velocity and, in a magnetoactive plasma, this can make a large

angle with the wave vector.

A particularly useful application of these ideas is to a graphical representation of the various types of wave modes that can propagate in a cold, magnetoactive plasma. This is known as the *Clemmow-Mullaly-Allis* or *CMA* diagram. The character of waves of a given frequency ω depends on the ratio of this frequency to the plasma freqency and the cyclotron freqency. This allows us to define two dimensionless numbers, $\omega_{pe}\omega_{pp}/\omega^2$ and $|\omega_{ce}|\omega_{cp}/\omega^2$. [Recall that $\omega_{pp} = \omega_{pe}\sqrt{m_e/m_p}$ and $\omega_{cp} = \omega_{ce}(m_e/m_p)$.] The space defined by these two dimensionless parameters can be subdivided into sixteen regions, within each of which the propagating modes have a distinctive character. The mode properties are indicated by sketching the topological form of the wave normal surfaces associated with each region.

The form of each wave-normal surface in each region can be deduced from the general dispersion relation (20.54). To deduce it, one must solve the dispersion relation for $1/\tilde{n} = \omega/kc = V_{\rm ph}/c$ as a function of θ and ω, and then generate the polar plot of $V_{\rm ph}(\theta)$.

On the CMA diagram's wave-normal curves the characters of the parallel and perpendicular modes are indicated by labels: R and L for right and left parallel modes ($\theta = 0$), and O and X for ordinary and extraordinary perpendicular modes ($\theta = \pi/2$). As one moves across a boundary from one region to another, there is often a change of which parallel mode gets deformed continuously, with increasing θ, into which perpendicular mode. In some regions a wave-normal surface has a figure-eight shape, indicating that the waves can propagate only over a limited range of angles, $\theta < \theta_{\rm max}$. In some regions there are two wave-normal surfaces, indicating that—at least in some directions θ—two modes can propagate; in other regions there is just one wave-normal surface, so only one mode can propagate; and in the bottom-right two regions there are no wave-normal surfaces, since no waves can propagate at these high densities and low magnetic-field strengths.

****

EXERCISES

Exercise 20.9 *Problem: Exploration of Modes in CMA Diagram*
For each of the following modes studied earlier in this chapter, identify in the CMA diagram the trajectory, as a function of frequency ω, and verify that the turning on and cutting off of the modes, and the relative speeds of the modes, are in accord with the CMA diagram's wave-normal curves.

a. EM modes in an unmagnetized plasma.

b. Left and right modes for parallel propagation in a magnetized plasma.

c. Ordinary and extraordinary modes for perpendicular propagation in a magnetized plasma.

Exercise 20.10 *Derivation: Refractive Index Surface*
Verify that the group velocity of a wave mode is perpendicular to the refractive index surface.

****

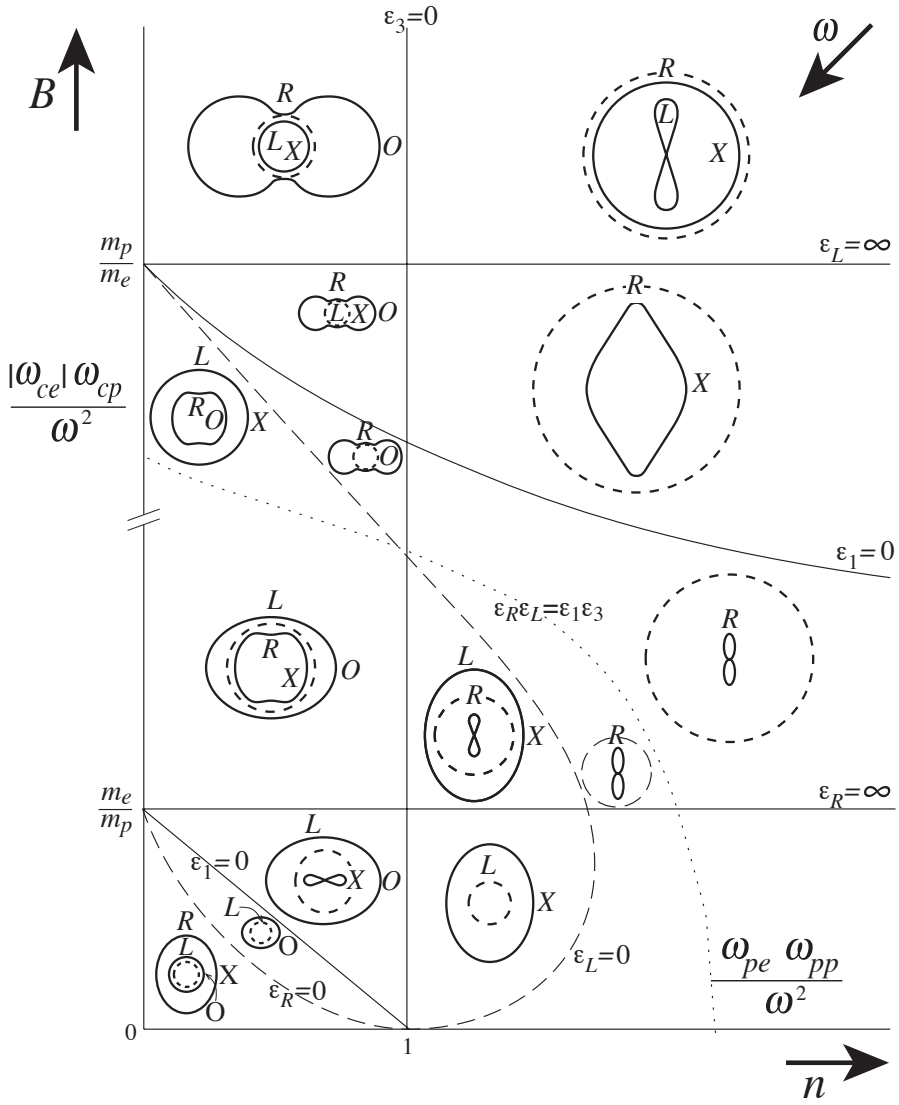

Fig. 20.7: Clemmow-Mullally-Allis (CMA) Diagram for wave modes of frequency ω propagating in a plasma with plasma frequencies ω_{pe}, ω_{pp} and gyro frequencies ω_{ce}, ω_{cp}. Plotted upward is the dimensionless quantity $|\omega_{ce}|\omega_{cp}/\omega^2$, which is proportional to B^2, so magnetic field strength also inreases upward. Plotted rightward is the dimensionless quantity $\omega_{pe}\omega_{pp}/\omega^2$, which is proportional to n^2, so the plasma number density also increases rightward. Since both the ordinate and the abscissa scale as $1/\omega^2$, ω increases in the left-down direction. This plane is split into sixteen regions by a set of curves on which various dielectric components have special values. In each of the sixteen regions is shown a wave-normal surface (phase-velocity surface at fixed ω; Fig. 20.6(a). It depicts the types of wave modes that can propagate for that region's values of frequency ω, magnetic field strength B, and electron number density n. In each wave-normal diagram the dashed circle indicates the speed of light; a point outside that circle has phase velocity greater than c; inside the circle, $V_{\rm ph} < c$. The topologies of the wave normal surfaces and speeds relative to c are constant throughout each of the sixteen regions, and change as one moves between regions.

20.7 Two Stream Instability

When considered on large enough scales, plasmas behave like fluids and are subject to a wide variety of fluid dynamical instabilities. However, as we are discovering, plasmas have internal degrees of freedom associated with their velocity distribution and this offers additional opportunities for unstable wave modes to grow and for free energy to be released. A full description of velocity-space instabilities is necessarily kinetic and must await the following chapter. However, it is instructive to consider a particularly simple example, the two stream instability, using cold plasma theory as this brings out several features of the more general theory in a particularly simple manner.

We will apply this theory in a slightly unusual way to the propagation of fast electron beams through the slowly outflowing solar wind. These electron beams are created by coronal disturbances generated on the surface of the sun (specifically those associated with "Type III" radio bursts). The observation of these fast electron beams was initially a puzzle because plasma physicists knew that they should be unstable to the exponential growth of electrostatic waves. What we will do in this section is demonstrate the problem. What we will not do is explain what is thought to be its resolution, since that involves nonlinear plasma physical considerations beyond the scope of this book.[1]

Consider a simple, cold (i.e. with negligible thermal motions) electron-proton plasma at rest. Ignore the protons for the moment. We can write the dispersion relation for electron plasma oscillations in the form

$$\frac{\omega_{pe}^2}{\omega^2} = 1. \tag{20.77}$$

Now allow the ions also to oscillate about their mean positions. The dispersion relation is slightly modified to

$$\frac{\omega_p^2}{\omega^2} = \frac{\omega_{pe}^2}{\omega^2} + \frac{\omega_{pp}^2}{\omega^2} = 1 \tag{20.78}$$

[cf. Eq. (20.21)]. If we added other components (for example Helium ions) that would simply add extra terms to the right hand side of Eq. (20.78).

Next, return to Eq. (20.77) and look at it in a reference frame through which the electrons are moving with speed u. The observed wave frequency must be Doppler-shifted and so the dispersion relation becomes

$$\frac{\omega_{pe}^2}{(\omega - ku)^2} = 1\ , \tag{20.79}$$

where ω is now the angular frequency measured in this new frame. It should be evident from this how to generalize Eq. (20.78) to the case of several cold streams moving with different speeds u_i. We simply add the terms associated with each component using angular frequencies that have been Doppler-shifted into the rest frames of the streams.

$$\boxed{\frac{\omega_{p1}^2}{(\omega - ku_1)^2} + \frac{\omega_{p2}^2}{(\omega - ku_2)^2} + \cdots = 1\ .} \tag{20.80}$$

(This procedure will be justified via kinetic theory in the next chapter.)

[1] *e.g.*Melrose, D. B. 1980

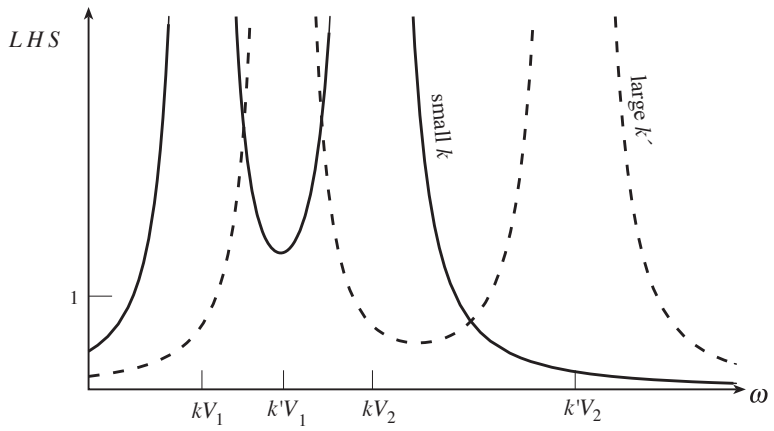

Fig. 20.8: Left hand side of the dispersion relation (20.80) for two cold plasma streams and two different choices of wave vector k. There are only two real roots for ω for small enough k.

The left hand side of the dispersion relation (20.80) is plotted in Fig. 20.8 for the case of two cold plasma streams. The dispersion relation (20.80) is a quartic in ω and so it should have four roots. However, for small enough k only two of these roots will be real; cf. Fig. 20.8. The remaining two roots must be a complex conjugate pair and the root with the positive imaginary part corresponds to a growing mode. We have therefore shown that for small enough k the two stream plasma will be unstable and small electrostatic disturbances will grow exponentially to large amplitude and ultimately react back upon the plasma. As we add more cold streams to the plasma, so we add more modes, some of which will be unstable. This simple example demonstrates how easy it is for a plasma to tap the free energy residing in anisotropic particle distribution functions.

Let us return to our original problem and work in the frame of the solar wind ($u_1 = 0$) where the plasma frequency is ω_p. If the beam density is a fraction α of the solar wind density so $\omega_{p2}^2 = \alpha\omega_{p1}^2$, and the beam velocity is $u_2 = V$, then by differentiating Eq. (20.80), we find that the local minimum of the left hand side is $\omega_p^2(1+\alpha^{1/3})^{1/2}/\omega^2$. This minimum exceeds unity for

$$k < \frac{\omega_p}{V}(1+\alpha^{1/3})^{3/2} \ . \tag{20.81}$$

This is therefore the condition for there to be a growing mode. The maximum value for the growth rate can be found simply by varying k. It is

$$\omega_i = \frac{3^{1/2}\alpha^{1/3}\omega_p}{2^{4/3}} \ . \tag{20.82}$$

For the solar wind near earth, we have $\omega_p \sim 10^5$rad s^{-1}, $\alpha \sim 10^{-3}$, $V \sim 10^4$km s^{-1}. We therefore find that the instability should grow in a length of 30km, much less than the distance from the sun which is 1.5×10^8 km! This describes the problem that we will not resolve.

****

EXERCISES

Exercise 20.11 *Derivation: Two stream instability*
Verify Eq. (20.82)

Exercise 20.12 *Example: Relativistic Two Stream Instabilty*
In a very strong magnetic field, we can consider electrons as constrained to move in one dimension along the direction of the magnetic field. Consider a beam of relativistic protons propagating with density n_b and speed $u_b \sim c$ through a cold electron-proton plasma along $\mathbf{B}$. Generalize the dispersion relation (20.80) for modes with $\mathbf{k} \parallel \mathbf{B}$.

Exercise 20.13 *Problem: Drift Waves*
Another type of wave mode that can be found from a fluid description of a plasma (but which requires a kinetic treatment to understand completely) is a *Drift wave*. The limiting case that we consider here is a modification of an ion acoustic mode in a strongly magnetized plasma with a density gradient. Suppose that the magnetic field is uniform and parallel to the direction $\mathbf{e}_z$. Let there be a gradient in the equilibrium density of both the electrons and the protons $n_0 = n_0(x)$. In the spirit of our description of ion acoustic modes in an unmagnetized, homogeneous plasma, (cf. Eq. (20.36)), treat the ion fluid as cold but allow the electrons to be warm and isothermal with temperature T_e. We seek modes of frequency ω propagating perpendicular to the density gradient, i.e. with $\mathbf{k} = (0, k_y, k_z)$.

(i) Consider the equilibrium of the warm electron fluid and show that there must be a fluid drift velocity along the direction $\mathbf{e}_y$ of magnitude

$$V_{de} = -\frac{V_{ia}^2}{\omega_{ci}} \frac{1}{n_0} \frac{dn_0}{dx} \ , \tag{20.83}$$

where $V_{ia} = (k_B T_e/m_p)^{1/2}$ is the ion acoustic speed. Explain in physical terms the origin of this drift and why we can ignore the equilibrium drift motion for the ions.

(ii) We will limit our attention to low frequency electrostatic modes that have phase velocities below the Alfvén speed. Under these circumstances, perturbations to the magnetic field can be ignored and the electric field can be written as $\mathbf{E} = -\boldsymbol{\nabla}\Phi$. Write down the three components of the linearized ion equation of motion in terms of the perturbation to the ion density n, the ion fluid velocity $\mathbf{u}$ and the electrostatic potential Φ.

(iii) Write down the linearized equation of ion continuity, including the gradient in n_0, and combine with the equation of motion to obtain an equation for the fractional ion density perturbation

$$\frac{\delta n}{n_0} = \left(\frac{(\omega_{cp}^2 k_z^2 - \omega^2 k^2) V_{ia}^2 + \omega_{cp}^2 \omega k_y V_{de}}{\omega^2 (\omega_{cp}^2 - \omega^2)} \right) \cdot \left(\frac{e\Phi}{k_B T_e} \right) \tag{20.84}$$

(iv) Argue that the fractional electron density perturbation follows a linearized Boltzmann distribution so that

$$\frac{\delta n_e}{n_0} = \frac{e\Phi}{k_B T_e} \ . \tag{20.85}$$

(v) Use both the ion and the electron density perturbations in Poisson's equation to obtain the electrostatic drift wave dispersion relation in the low frequency ($\omega \ll \omega_{cp}$), long wavelength ($k\lambda_D \ll 1$) limit:

$$\omega = \frac{k_y V_{de}}{2} \pm \frac{1}{2}[k_y^2 V_{de}^2 + 4k_z^2 V_{ia}^2]^{1/2} \ . \tag{20.86}$$

Describe the physical character of the mode in the additional limit $k_z \to 0$. A proper justification of this procedure requires a kinetic treatment which also shows that, under some circumstances, drift waves can be unstable and grow exponentially. Just as the two stream instability provides a mechanism for plasmas to erase non-uniformity in velocity space, so drift waves can rapidly remove spatial irregularities.

****

Bibliographic Note

The definitive monograph on waves in plasmas is Stix (1992). For the most elementary textbook treatment see portions of Chen (1974). For more sophisticated and detailed textbook treatments see Boyd and Sanderson (1969), Clemmow and Doughtery (1969), Krall and Trivelpiece (1973), Landau and Lifshitz (1981), and Schmidt (1966). For treatments that focus on astrophysical plasmas, see Melrose (1980) and Parks (1991).

Bibliography

Boyd, T. J. M. & Sanderson, J. J. 1969. *Plasma Dynamics*, London: Nelson.

Chen, F. F. 1974. *Introduction to Plasma Physics*, New York: Plenum.

Clemmow, P. C. & Dougherty, J. P. 1969. *Electrodynamics of Particles and Plasmas*, Reading: Addison-Wesley.

Krall, N. A. & Trivelpiece, A. W. 1973. *Principles of Plasma Physics*, New York: McGraw-Hill.

Landau, L. D. & Lifshitz, E. M. 1981. *Plasma Kinetics*, Oxford: Pergamon.

Melrose, D. B. 1980. *Plasma Astrophysics*, New York: Gordon and Breach.

Parks, G. K. 1991. *Physics of Space Plasmas*, Redwood City: Addison-Wesley.

Schmidt, G. 1966. *Physics of High Temperature Plasmas*, New York: Academic.

Stix, T. H. 1992. *Waves in Plasmas*, New York: American Institute of Physics.

Box 20.2
Important Concepts in Chapter 20

- For a linear dielectric medium: polarization vector $\mathbf{P}$, electrical susceptibility tensor χ_{ij}, dielectric tensor ϵ_{ij}, electrical conductivity tensor $\kappa_{\mathbf{e}\,ij}$, wave operator in Fourier domain L_{ij}, and dispersion relation $\det||L_{ij}|| = 0$, Sec. 20.2
- Two-fluid formalism for a plasma: for each species – fluid velocity $\mathbf{u}_s = \langle \mathbf{v}_s \rangle$, pressure tensor $\mathbf{P}_s$, particle conservation, and equation of motion (Euler equation plus Lorentz force), Sec. 20.3.1
- Waves in cold, unmagnetized plasma, Secs. 20.3.2, 20.3.3
  - How to deduce the electric field and particle motions in a wave mode, Secs. 20.3.2, 20.3.4
  - Electromagnetic waves and their cutoff at the plasma frequency, Secs. 20.3.3, 20.3.5
  - Nonpropagating electrostatic oscillations, Sec. 20.3.2
- Waves in warm, unmagnetized plasma:
  - Electrostatic oscillations become Langmuir waves, Sec. 20.3.4
  - Ion acoustic waves, Sec. 20.3.4
- *Cutoff:* form of dispersion relation near a cutoff; Electromagnetic waves and Langmuir waves as examples; for inhomogeneous plasma: deflection of wave away from cutoff region in space, Secs. 20.3.5, 20.5
- *Resonance:* form of dispersion relation near a resonance; Ion acoustic waves as example; for inhomogeneous plasma: attraction of wave into resonance region and dissipation there, Secs. 20.3.5, 20.5
- Waves in cold, magnetized plasma, Sec. 20.4
  - Waves propagating parallel to the magnetic field: Alfven waves, whistlers, right-circurlarly-polarized EM waves, and left-circularly-polarized EM waves, Sec. 20.4.2
  - Waves propagating perpendicular to the magnetic field: Magnetosonic waves, upper hybrid waves, lower hybrid waves, ordinary EM waves, extraordinary EM waves, Sec. 20.4.3
  - Ways to depict dependence of phase velocity on direction: phase-velocity (or wave-normal) surface and CMA diagram based on it; refractive index surface, Sec. 20.6
- Two-stream instability, Sec. 20.7